Soft Skin Texture Modulation for Social Robotics

Yuhan Hu[1], Zhengnan Zhao[1], Abheek Vimal[1], and Guy Hoffman[1]

***Abstract*— Robots designed for social interaction often express their internal and emotional states through nonverbal behavior. In most systems, this is achieved using facial expressions, gestures, locomotion, and tone of voice. In this paper, we propose a new expressive nonverbal channel for social robots in the form of a texture-changing skin. Our approach is inspired by biological systems, which frequently display their internal states through skin texture change. We present two designs for soft fluidic Texture Units (TU): goosebumps and spikes, and a design for an interleaved TU array that can function as an expressive social robot skin. We discuss fabrication, actuation, and control considerations, as well as a framework for mapping emotional states to texture changes. We exemplify the design in a social robot which has both a screen-projected face and the proposed texture-changing expressive skin.**

I. Introduction

Internal and affective state expression is at the core of social robotics [1]–[3]. To express these states, the vast majority of social robots use body movement (kinesics) [4]–[6], facial expressions [7], [8], and expressive locomotion [9]. In some cases, robots modulate their tone of voice (vocalics) to express emotional states or intentional context [4], [10].

These nonverbal modalities are inspired by human and animal modes of nonverbal expression, but many biological systems also display changes to their skin texture to express fear, excitement, and other emotional states [11]. Some examples include: human goosebumps, cats' neck fur raising, dogs' back hair, the needles of a porcupine, spiking of a blowfish, or a bird's ruffled feathers. This widespread and easily readable behavior has thus far not been utilized for expressive behavior in social robotics.

Recent developments in soft robotics enable the implementation of skin changes in social robots. Doing so can increase the spectrum of expressive capabilities. Skin change is a particularly useful communication channel since it operates on two channels: It is perceived not only visually, but also haptically, if the human is holding or touching the robot.

In this work, we describe a system for social robots to express their internal state using skin texture changes. We present the following: (1) a design for a texture changing skin for social robots in the form of an interleaved fluidic network of texture units (TUs) (Fig. 1); (2) two alternative systems for the actuation and control of the TU arrays; (3) a framework mapping emotional states to texture changes; and (4) a prototype for a social robot that has both facial expressions and the proposed texture-changing skin (Fig. 2).

[1]The authors are with the Sibley School of Mechanical and Aerospace Engineering, Cornell University, Ithaca, NY, USA {yh758,hoffman}@cornell.edu

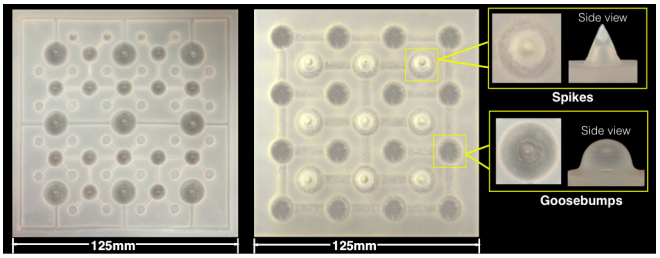

Fig. 1. Two socially expressive Texture Modules: multi-scale Goosebump Texture Units (TUs) (left) and a mixture of Goosebump and Spike TUs. Each set of TUs is controlled separately via a fluidic conduit network.

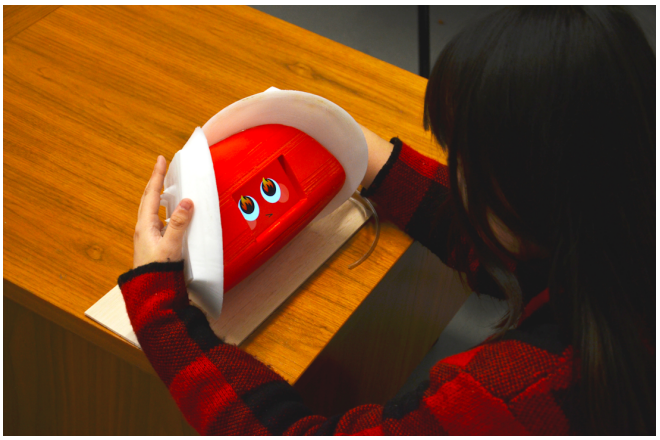

Fig. 2. A social robot prototype combining facial expression and the texture changing skin. During human-robot interaction, the user puts their palms on the shells for haptic feedback and makes eye contact with the screen face.

II. Related Work

Our work relates to the literature in social robot nonverbal expression, soft social robots, and texture change in soft robotics.

A. Nonverbal Expression in Social Robots

One of the most important capacities of social robots is to generate nonverbal behaviors to support social interaction [1]–[3]. Humans and animals have a wide variety of modalities to express emotional and internal states for interaction [11], but in robotics these have been studied unequally, with a heavy focus on kinesics, facial expression, gaze, locomotion, and vocalics [4]–[10]. Examples of robots using gestures and facial expressions abound, including Probo [12], KOBIAN [13], Simon [14], iCat [15], and Sparky [16]. A fraction of social robots do use touch as a communication mode, e.g., the "Huggable" robot [17], handshaking robots [18], and CuddleBits [19]. In all of these

cases, however, the robot only detects touch, but reacts with a whole-body movement. None of these robots change their skin texture as an expressive channel.

B. Soft Social Robots

In recent years, soft materials have been explored in social robot design. The common design of these robots consists of a soft shell over a rigid inner mechanism. Examples include Dragonbot [20], a fur covered socially expressive robot platform with a mobile phone face; Keepon [21] a rigid linkage mechanism covered by a silicone exterior; and Tofu [22], a winch mechanism embedded in a compressive foam structure. The skins of many of these soft social robots are made of silicon or artificial fur. They express their internal state through the movement and deformation of this exterior skin, but the texture of the skins does not change. Texture change thus remains an unexplored expressive channel for socially interactive robots.

C. Texture Change in Soft Robots

At the same time, there are a number of new methods for controlling soft material surface shapes, varying from pneumatic actuation [23], shape memory polymers [24], liquid crystal elastomers [25], and more [26]. Of particular relevance is a recently introduced programmable 3D shape approach, which provides a systematic method of transforming 2D planar surface to target 3D shapes [27]. This technique uses an inextensible mesh embedded inside an elastomer membrane, and a computational design method to map 3D target shapes to the 2D planar surfaces. A similar method can be used for designing a social robot skin that uses texture change for expression.

III. Texture Design And Fabrication

The aim of this work is to develop a soft robotic skin that can be modulated to express emotions and other internal states through texture change. We present two forms of expressive texture change inspired by skin texture changes appearing in nature: goosebumps and spikes. We chose these two forms as an initial exploration because they are often associated with positive and negative emotion expression in people and animals. At the core of our design is a fluid-actuated multi-layer elastomer skin, which changes its surface texture in response to pressure. To generate these textures, we modeled the skin as an array of *Texture Units*.

A. Texture Unit Design

A Texture Unit (TU) is the minimal element of the texture-changing skin. It is designed to be both visually and haptically expressive. Each TU has a specifically designed shape, which includes an elastomer body, a cavity inside the elastomer, reinforcement layers of inextensible films, and optional embedded haptic-expressive rigid elements (Fig. 3). The diameter was chosen to be between 10–20mm, so that multiple texture types can fit under a single palm and affect the expression as a group. The shape of the cavities, the shape and placement of the inextensible films, and the shape and placement of the rigid elements results in TU types with different responses. To illustrate this, we provide two examples of Texture Unit designs: Goosebumps and Spikes. More complex TUs can be designed using computational methods as exemplified in [27].

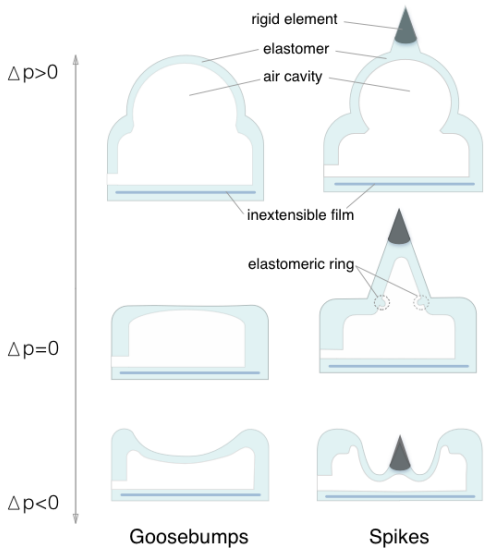

Fig. 3. The Goosebump TU (left) is composed of an elastomer body, a column shaped cavity, and an inextensible film. It transforms from a flat initial surface to a smooth bump under positive pressure, and a slight dent under negative pressure. The Spike TU (right) is composed of a conical upper spike, a cylindrical bottom cavity, a body with a centrally positioned elastomer ring, an inextensible film, and a rigid element embedded in the tip for added haptic expression. It hides its sharp tip in the dent under negative pressure and deforms into a thorn under positive pressure.

1) Goosebump: The Goosebump TU (TU-GB) contains an inner cavity in the shape of a column with a slightly rounded top, and without any rigid elements attached. A layer of inextensible film covering the whole TU-GB footprint is embedded below the cavity to constrain the downwards deformation. The TU-GB transforms from an initial flat

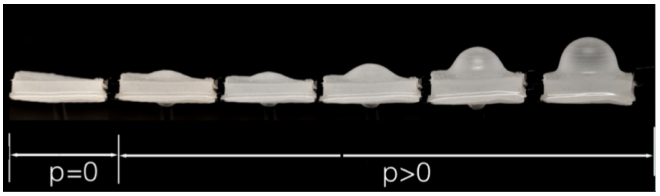

Fig. 4. Inflating of a TU-GB from 0 to positive pressure results in transition from a flat surface to an increasingly large bump.

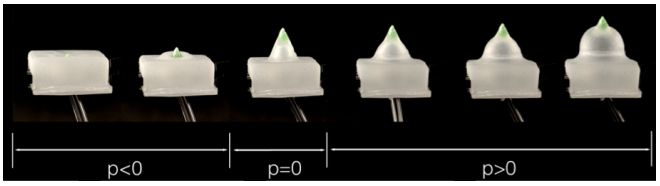

Fig. 5. Inflation process of a TU-S from negative pressure with the rigid tip hidden in a dent, to positive pressure with a haptic protruding thorn.

surface to a smooth bump under inflation, and to a slight dent under deflation (Fig. 3 (left) and Fig. 4).

2) Spike: The Spike TU (TU-S) is structured as a two-chamber design: a conical upper spike chamber above a column-shaped chamber; an elastomer ring at the interface between the two chambers to constrain radial deformation; and a rigid element on the tip of the TU-S made of Polylactic acid (PLA), featuring a sharp tip for both visual and haptic expression. The TU-S is proportioned so that the sharp tip is hidden in the dent under negative pressure, but is deformed to a thorn under positive pressure (Fig. 3 right and Fig. 5).

B. Combining TUs to Form Texture Modules

To achieve a variety of visual and haptic experiences, we lay out a matrix of TUs. Ideally, we would want to control each TU separately; in practice, this would complicate the actuation and control of the robot to the point of infeasibility. This problem is further exacerbated in the context of social robotics, where component size is a consideration. To avoid distraction from the interaction, we aim for self-contained actuation. Noise is also a concern, as social interaction can be highly affected by noise [28], a consideration of increasing concern in human-robot interaction [29].

The design of a large number of actuated units with self-contained actuation and a low noise profile is difficult given the inherent limitations of fluidic actuators. We balance this trade-off by interleaving two 2D arrays of texture units into a single Texture Module (TM), with inner fluidic chambers connecting TUs of the same array . We illustrate the flexibility of this design by using both TU types, as well as varying the size and shape of the TUs within a single module:

1) Multi-Scale TU-GB: The first Texture Module (Fig.1 left) combines TU-GB elements of different sizes (15mm, 10mm, and 6mm diameter). All 15mm TU-GBs are connected to one fluidic network and all 10mm and 6mm TU-GBs are connected to another fluidic network. Each network can be separately actuated. The visual and haptic experiences of the two groups can be differentiated by the TUs' sizes and placements.

2) Mixture of TU-GB and TU-S: The second TM (Fig.1 right) combines TU-GB and TU-S elements of the same size (15mm diameters). We again link the TUs using two fluidic conduit networks, each connecting one type of TU. By separately controlling each group we can create both visually and haptically distinct expressions.

C. Texture Module Fabrication

The main body of the texture skin is made of an extensible elastomer (Smooth-on Ecoflex 00-30), using a mold-casting fabricating process. A plastic positive of the inner cavity and fluidic channels is fabricated using 3D-printed PLA and fixed in a mold box. The elastomer is molded to fabricate the upper part of the cavities, as shown in Fig. 6(a–b). The bottom layer is fabricated with an inextensible film embedded in it (Fig. 6(c)) and the cured upper part is attached to the bottom layer to form the closed cavities. For the TU-GB/TU-S mixed module, we use two parts to make the mold, one for casting the outer shape (Fig. 6(d) left), the other for fluidic cavity and chamber (Fig. 6(d) right). Before casting the top layer, we embed the rigid elements of the spikes (Fig. 6(e–f)). We use the same method as in the Fig.6(c) to fabricate the bottom layer in the pre-cured elastomer with the embedded inextensible film.

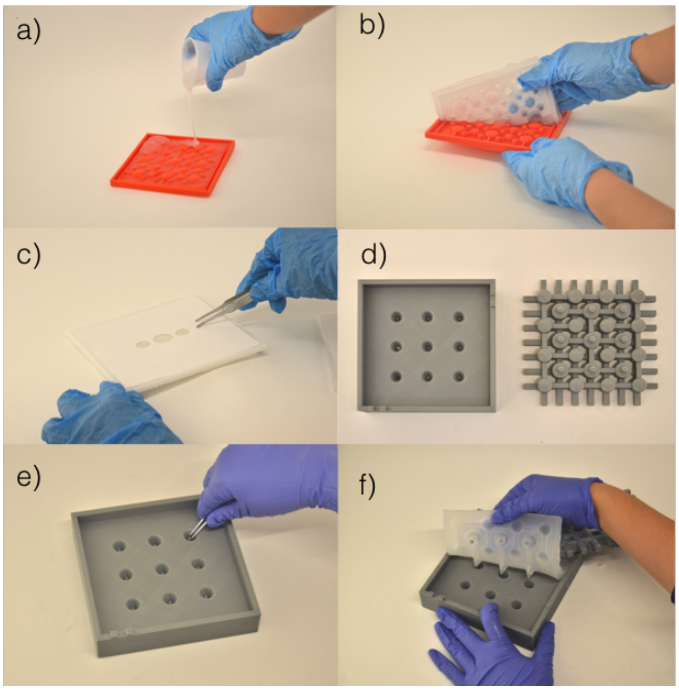

Fig. 6. Fabrication process of the Texture Modules (TM). To fabricate the multi-scale TU-GB, a mold of the positive of cavities and conduits is 3D printed and the elastomer is poured to fabricate the upper part (a–b). The bottom layer is fabricated with an inextensible film embedded in it, and attached to the upper part before it is cured (c). For the TU-GB and TU-S mixture TM, the mold is composed of two parts (d). Rigid elements are embedded into the mold for the haptically expressive tips (e–f).

IV. Fluidic System Control

The application domain of social interaction necessitates special consideration to the actuation of the texture, as both size and noise are of importance when interacting with humans. We present and compare two actuation systems used for actuating a TM, designed around two different power sources: a more commonly used method of rotary displacement pumps with pressure-feedback solenoid valve control, and an alternative power screw controlled linear displacement pump with no feedback control.

A. Rotary Displacement Pump with Solenoid Valves

A common way to actuate robots based on fluidic elastomer cavities is using a source of pressure, often in the form of a rotary displacement pump, and control the pressure with an array of solenoid valves and pressure sensors [30]. In our system, we used two separate control circuits, each with one pump, two solenoid valves, and a pressure sensor for feedback control (Fig. 7 top). In the experiments described below, we use a 12V air pump with a $0 - 32$ psi pressure range as the power source of the system. To control the pump

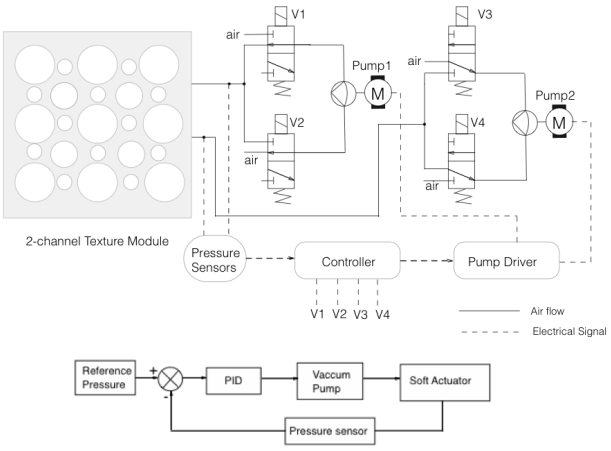

Fig. 7. An actuation system composed of one rotary displacement pump, two solenoid valves, and a pressure sensor for each channel (top). The system uses PID closed-loop control with the pressure sensor output as the feedback signal (bottom).

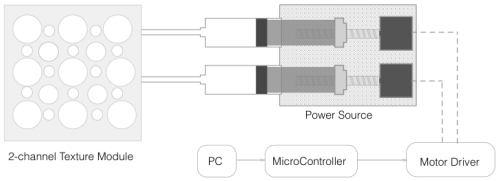

Fig. 8. The open-loop system with linear displacement pumps is composed of a soft texture module, two pumps, and a micro-controller with a stepper motor driver.

flow to inflate or deflate the device, we use an H-bridge-like circuit layout in combination with a pulse-width-modulation (PWM) signal. The PWM signal sets the positive or negative flow rate. The pressure sensors are used as feedback for a PID closed-loop control of the system (Fig. 7 bottom).

After implementing this to control for a variety of texture states, we identified several issues with this design:

1) **Response time —** RT is limited by the solenoid response time, the accuracy of the pressure sensor and the length and diameter of the tube.
2) **Control accuracy—** Accuracy is low, as determined by the precision of the pressure sensor.
3) **Efficiency —** The system is inefficient because of the loss of air through leakage and exhaust. In addition, the system needs to spend energy just to hold position.
4) **Noise —** The rotary pump as the power source and the solenoid switches are noisy and distracting.

B. Power Screw Actuated Linear Displacement Pump

To overcome issues mentioned above, we switched to a linear displacement design driven by power screws. The new design is based on a re-purposed syringe, resulting in a cylindrical pump with a plunger, which is displaced by a stepper motor driving a power screw. Due to the negligible leakage we experienced in tests, the precision of the stepper

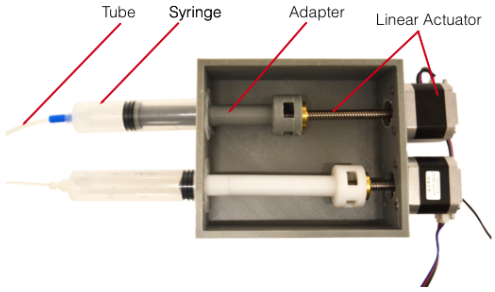

Fig. 9. Each linear displacement pump consists of a re-purposed syringe linked with a linear stepper motor through a custom designed adapter.

motor, and the predictable volume displacement, this design also allows us to use open-loop volume control.

The resulting system is composed of a soft texture module with fluidic actuators, two pumps, and a micro-controller with a stepper driver. (Fig. 8) We use a NEMA-17 stepper motor with $1.8\,\mathrm{deg}$ step size, $40Ncm$ holding torque, and a phase inductance of $3.8mH$) attached to a 4-start Acme screw, resulting in a top linear speed of $100mm/s$. The screw is driving a 30ml syringe. The plunger is custom-designed to connect the thread nut and the piston. (Fig. 9).

V. System Evaluation

The new actuation system has the benefit of lower audible noise levels and a compact size, but it does not have feedback control for pressure, an important factor of haptic interaction. This is further exacerbated by the fact that the fluidic enclosure of each TU can expand. We thus need to evaluate its mechanical properties including deformation and pressure changes as a response to volume changes. This can then allow us to calibrate the deformation and pressure corresponding to the motor control signals.

A. TU Experiments

To characterize the TUs, we performed inflating and deflating tests to determine the relationship between the supplied volume V, the displacement of the central point z, and the fluidic chamber pressure p. In these tests, we use air as the actuating fluid, and TU-GB and TU-S samples of 15mm diameter each. We pressurize and depressurize the sample over 5 cycles, and present mean values. Fig. 10 shows the setup and results of these tests.

B. TM Experiments

To calibrate Texture Module (TM) deformation corresponding to the motor control signals, we use a TU-GB/TU-S mixture TM as the experiment sample. We measured the the fluidic chamber pressure p and the volume of the displaced fluid V. The deformation of the TM are shown in Fig.11 with discretized values of pressure modes for each of the two channels. G and S indicate the TU–GB and TU-S channels respectively, and "-" "0" "+" "++" indicate the negative, zero, or positive chamber pressures. Using air as the fluid, these correspond to $[-0.9, 0, 0.9, 1.5]$ psi for the TU-GB submodule and $[-0.7, 0, 1.1]$ psi for the TU-S submodule.

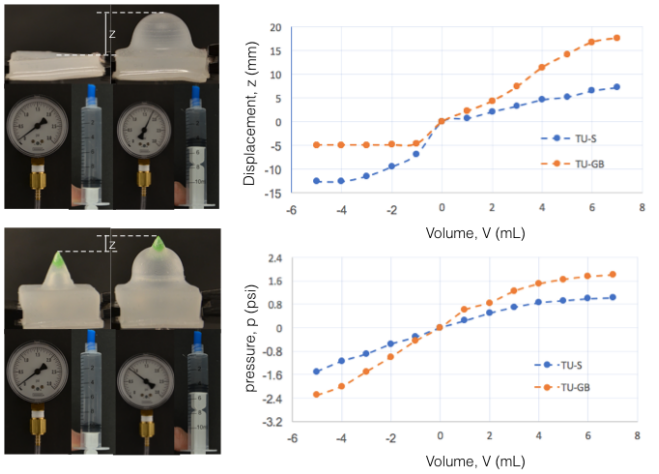

Fig. 10. Experiment setup of TU deformation measuring the displacement z, the supplied volume V, and the chamber pressure p using air as the actuating fluid (left). The experiment result shows the relationship between z and V, and p and V in the TU-GB and TU-S deformation process (right).

VI. Application: Emotion to Texture

To illustrate the application of our system to social robots, we propose a possible mapping between the control signals of the TM and the robot's internal emotional state.

A. Mapping Emotions to Texture Change

In social and cognitive psychology, a common model for emotional state is Russell's circumplex model of emotions [31]. This model is often used in the affective computing literature in its 2D version, where each point of the plane corresponds to an emotional state [32]. The two dimensional scales are Valence (positive / negative) and Arousal (high / low). Each emotional state is expressed by a linear combination of these two dimensions. Fig. 12 shows some common emotions mapped onto the circumplex model.

We propose to map the emotion plane to control variables of texture change, including shape, texture change frequencies and amplitudes, as follows: The amplitude of the TUs represents valence, with negative valence mapping to the TU-Ss and positive to the TU-GBs. This is inspired by natural responses, where spikes deliver an unpleasant haptic experience and represent a defensive state, and goosebumps are associated with pleasure and excitement. We then use the texture change frequency to represent the emotional Arousal dimension. Fig. 12 shows an abstracted mapping between the texture change space and the emotion plane.

B. Robot Appearance Design

As a final step, we present an oyster-like robotic prototype including two TM shells and a screen-projected face (Fig. 13). While interacting with the robot, the user sits in front of the robot, puts their palms on the haptic shells with eyes focused on the robot's expressive face (Fig. 2). The robot can interact with the user by showing an emotion-expressive face, with an emotion-mapped texture change applied to the haptic channel for additional expressive capability. We are currently using this robot in a research study

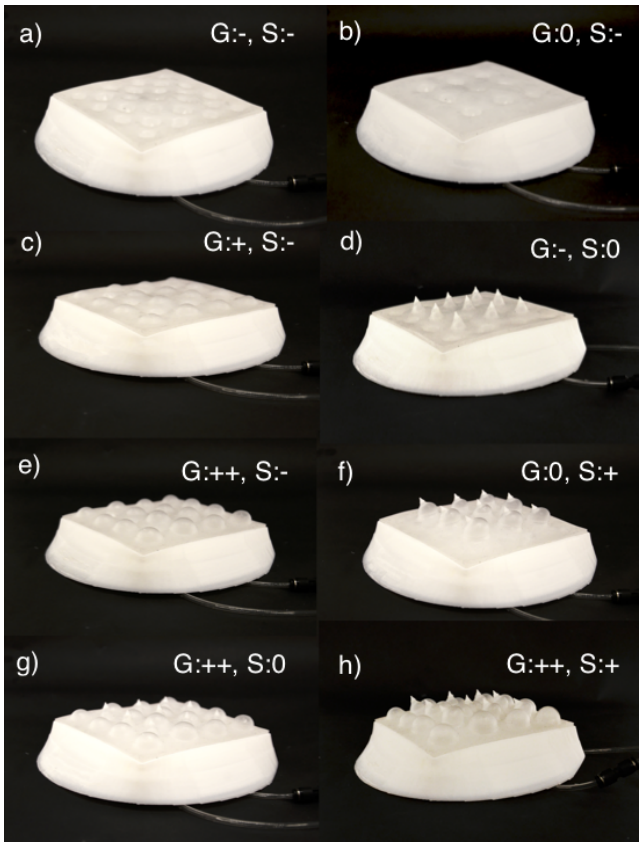

Fig. 11. Deformation of mixed TU-GB / TU-S TM in response to the change of chamber pressure, where G and S indicates the TU-GB and TU-S channel respectively, and the symbols "-" "0" "+" "++" represent the level of p of each channel on a texture module (TU-GB: $[-0.9, 0, 0.9, 1.5]$ psi; TU-S: $[-0.7, 0, 1.1]$ psi).

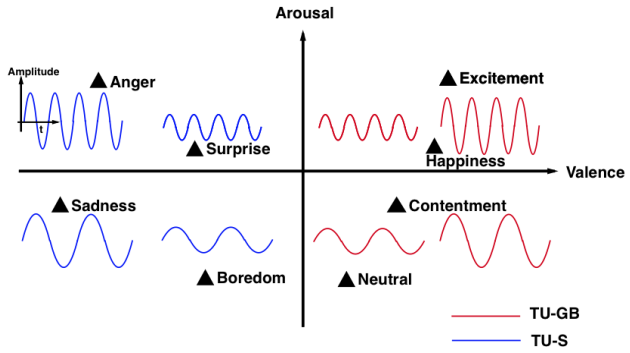

Fig. 12. Russell's circumplex model of emotion with a mapping of TU control to the 2D emotion plane. TU-G are activated on the positive valence side of the emotion plane, and TU-S for the negative valence side. The amplitude of texture changing quantifies the absolute value of the Valence dimension; the frequency of change is mapped to the Arousal dimension.

to evaluate the differences in expressive capacity between facial expressions and texture change.

VII. Conclusion

In this paper, we presented a design of a soft texture changing skin for social robotics, inspired by the common animal phenomenon of raising dermal structures as a response to

Fig. 13. The oyster-like structure is composed of two texture changing shells and an expressive screen-projected face.

internal and emotional state changes. We demonstrated the design and fabrication of single texture units (TUs), including smooth TUs and TUs embedded with rigid haptic elements. We then presented the design of interleaved modules of TUs with separately controllable fluidic conduits. We discussed actuation and control with social robotics considerations, such as size and noise, and integrated the proposed design in a social robot prototype. Future work remains to evaluate the human-robot interaction effects of this expressive modality, and to compare it to existing modalities, most notably facial expressions. We would also like to explore additional TU types and TM arrangements, and study ways to make the social robot design self-contained.

At the moment, most social robots express internal state only by using facial expressions and gestures. We believe that the integration of a texture-changing skin, combining both haptic and visual modalities, can thus significantly enhance the expressive spectrum of robots for social interaction.

References

[1] T. Fong, I. Nourbakhsh, and K. Dautenhahn, "A survey of socially interactive robots," *Robotics and autonomous systems*, vol. 42, no. 3, pp. 143–166, 2003.

[2] M. A. Goodrich and A. C. Schultz, "Human-robot interaction: a survey," *Foundations and trends in human-computer interaction*, vol. 1, no. 3, pp. 203–275, 2007.

[3] C. Breazeal, K. Dautenhahn, and T. Kanda, "Social robotics," in *Springer Handbook of Robotics*. Springer, 2016, pp. 1935–1972.

[4] A. Thomaz, G. Hoffman, M. Cakmak, *et al.*, "Computational human-robot interaction," *Foundations and Trends® in Robotics*, vol. 4, no. 2-3, pp. 105–223, 2016.

[5] C.-M. Huang and B. Mutlu, "Modeling and evaluating narrative gestures for humanlike robots." in *Robotics: Science and Systems*, 2013, pp. 57–64.

[6] H. Admoni, A. Dragan, S. S. Srinivasa, and B. Scassellati, "Deliberate delays during robot-to-human handovers improve compliance with gaze communication," in *Proc of the 2014 ACM/IEEE international conference on Human-robot interaction*. ACM, 2014, pp. 49–56.

[7] R. Gockley, A. Bruce, J. Forlizzi, M. Michalowski, A. Mundell, S. Rosenthal, B. Sellner, R. Simmons, K. Snipes, A. C. Schultz, *et al.*, "Designing robots for long-term social interaction," in *Intelligent Robots and Systems, 2005.(IROS 2005). 2005 IEEE/RSJ International Conference on*. IEEE, 2005, pp. 1338–1343.

[8] C. C. Bennett and S. Šabanović, "Deriving minimal features for human-like facial expressions in robotic faces," *International Journal of Social Robotics*, vol. 6, no. 3, pp. 367–381, 2014.

[9] H. Knight and R. Simmons, "Expressive motion with x, y and theta: Laban effort features for mobile robots," in *Robot and Human Interactive Communication, 2014 RO-MAN: The 23rd IEEE International Symposium on*, Aug 2014, pp. 267–273.

[10] A. Niculescu, B. van Dijk, A. Nijholt, H. Li, and S. L. See, "Making social robots more attractive: the effects of voice pitch, humor and empathy," *International journal of social robotics*, vol. 5, no. 2, pp. 171–191, 2013.

[11] C. Darwin, *The expression of the emotions in man and animals*. University of Chicago press, 1965, vol. 526.

[12] J. Saldien, K. Goris, B. Vanderborght, J. Vanderfaeillie, and D. Lefeber, "Expressing emotions with the social robot probo," *International Journal of Social Robotics*, vol. 2, no. 4, pp. 377–389, 2010.

[13] M. Zecca, Y. Mizoguchi, K. Endo, F. Iida, Y. Kawabata, N. Endo, K. Itoh, and A. Takanishi, "Whole body emotion expressions for kobian humanoid robotpreliminary experiments with different emotional patterns," in *IEEE International Symposium on Robot and Human Interactive Communication*. IEEE, 2009, pp. 381–386.

[14] M. Cakmak, C. Chao, and A. L. Thomaz, "Designing interactions for robot active learners," *IEEE Transactions on Autonomous Mental Development*, vol. 2, no. 2, pp. 108–118, 2010.

[15] A. van Breemen, X. Yan, and B. Meerbeek, "icat: an animated user-interface robot with personality," in *Proceedings of the fourth international joint conference on Autonomous agents and multiagent systems*. ACM, 2005, pp. 143–144.

[16] M. Scheeff, J. Pinto, K. Rahardja, S. Snibbe, and R. Tow, "Experiences with sparky, a social robot," in *Socially Intelligent Agents*. Springer, 2002, pp. 173–180.

[17] W. D. Stiehl, J. Lieberman, C. Breazeal, L. Basel, L. Lalla, and M. Wolf, "Design of a therapeutic robotic companion for relational, affective touch," in *IEEE International Workshop on Robot and Human Interactive Communication*. IEEE, 2005, pp. 408–415.

[18] C. Bevan and D. Stanton Fraser, "Shaking hands and cooperation in tele-present human-robot negotiation," in *Proceedings of the Tenth Annual ACM/IEEE International Conference on Human-Robot Interaction*. ACM, 2015, pp. 247–254.

[19] P. Bucci, X. L. Cang, A. Valair, D. Marino, L. Tseng, M. Jung, J. Rantala, O. S. Schneider, and K. E. MacLean, "Sketching cuddlebits: Coupled prototyping of body and behaviour for an affective robot pet," in *Proceedings of the 2017 CHI Conference on Human Factors in Computing Systems*. ACM, 2017, pp. 3681–3692.

[20] A. A. M. Setapen, "Creating robotic characters for long-term interaction," Ph.D. dissertation, Massachusetts Institute of Technology, 2012.

[21] H. Kozima, M. P. Michalowski, and C. Nakagawa, "Keepon," *International Journal of Social Robotics*, vol. 1, no. 1, pp. 3–18, 2009.

[22] R. Wistort and C. Breazeal, "Tofu: a socially expressive robot character for child interaction," in *Proc of the 8th International Conference on Interaction Design and Children*. ACM, 2009, pp. 292–293.

[23] B. Mosadegh, P. Polygerinos, C. Keplinger, S. Wennstedt, R. F. Shepherd, U. Gupta, J. Shim, K. Bertoldi, C. J. Walsh, and G. M. Whitesides, "Pneumatic networks for soft robotics that actuate rapidly," *Advanced Functional Materials*, vol. 24, no. 15, pp. 2163–2170, 2014.

[24] Q. Ge, A. H. Sakhaei, H. Lee, C. K. Dunn, N. X. Fang, and M. L. Dunn, "Multimaterial 4d printing with tailorable shape memory polymers," *Scientific reports*, vol. 6, p. 31110, 2016.

[25] T. H. Ware, M. E. McConney, J. J. Wie, V. P. Tondiglia, and T. J. White, "Voxelated liquid crystal elastomers," *Science*, vol. 347, no. 6225, pp. 982–984, 2015.

[26] C. Yu, Z. Duan, P. Yuan, Y. Li, Y. Su, X. Zhang, Y. Pan, L. L. Dai, R. G. Nuzzo, Y. Huang, *et al.*, "Electronically programmable, reversible shape change in two-and three-dimensional hydrogel structures," *Advanced Materials*, vol. 25, no. 11, pp. 1541–1546, 2013.

[27] J. Pikul, S. Li, H. Bai, R. Hanlon, I. Cohen, and R. Shepherd, "Stretchable surfaces with programmable 3d texture morphing for synthetic camouflaging skins," *Science*, vol. 358, no. 6360, pp. 210–214, 2017.

[28] L. Langeveld, R. van Egmond, R. Jansen, and E. Ozcan, "Product sound design: Intentional and consequential sounds," in *Advances in industrial design engineering*. InTech, 2013.

[29] D. Moore, H. Tennent, N. Martelaro, and W. Ju, "Making noise intentional: A study of servo sound perception," in *Proceedings of the 2017 ACM/IEEE International Conference on Human-Robot Interaction*. ACM, 2017, pp. 12–21.

[30] K. Suzumori, S. Iikura, and H. Tanaka, "Applying a flexible microactuator to robotic mechanisms," *IEEE control systems*, vol. 12, no. 1, pp. 21–27, 1992.

[31] J. A. Russell and M. Bullock, "Multidimensional scaling of emotional facial expressions: similarity from preschoolers to adults." *Journal of Personality and Social Psychology*, vol. 48, no. 5, p. 1290, 1985.

[32] A. Hanjalic and L.-Q. Xu, "Affective video content representation and modeling," *IEEE Transactions on multimedia*, vol. 7, no. 1, pp. 143–154, 2005.